

# Wooden Sleeper Decayed Detection for Rural Railway Prognostics Using Unsupervised Deeper FCDDs

Takato Yasuno<sup>1</sup>, Masahiro Okano<sup>1</sup>, and Junichiro Fujii<sup>1</sup>

<sup>1</sup> *Yachiyo Engineering, Co.,Ltd., Tokyo, Taito-ku, 111-8648, Japan*  
*tk-yasuno@yachiyo-eng.co.jp*  
*ms-okano@yachiyo-eng.co.jp*  
*jn-fujii@yachiyo-eng.co.jp*

## ABSTRACT

It is critical for railway managers to maintain a high standard to ensure user safety during daily operations. Top-view or side-view cameras and GPS positioning system have enabled progress toward automating the periodic inspection of defective features and assessing the deteriorated status of the railway components. Frequently, collecting deteriorated status data constraints time consuming and repeated data acquisition, because the temporal occurrence is extremely imbalanced. Supervised learning approach requires thousands of paired dataset of defective raw images and annotated labels. However, one-class classification approach has a merit that fewer images enables us to optimize the parameters for training normal and anomalous feature. Simultaneously, the visual heat map explanation enables us to discriminate the localized damage feature. In this paper, we propose a prognostic discriminator pipeline to automate one-class damage classification towards defective railway components. We also sensitivity analyze toward the backbone and the receptive field based on convolutional neural networks (CNNs) using pre-trained networks: baseline CNN27, VGG16, ResNet101, and Inception Networks. We also visualize the explanation of the defective railway feature using a transposed Gaussian up-sampling. We demonstrate our application for railway inspection in an open-accessed dataset of defective railway components, and wooden sleeper deterioration in rural railway. The heatmap is so important that the hazard-marks could cause an operational delay, an urgent inspection, and unexpected accident to passenger impact in railway inspection. Furthermore, we mention its usability for prognostic monitoring and future works for railway components inspection in the predictive maintenance of railway systems.

Takato Yasuno et al. This is an open-access article distributed under the terms of the Creative Commons Attribution 3.0 United States License, which permits unrestricted use, distribution, and reproduction in any medium, provided the original author and source are credited.

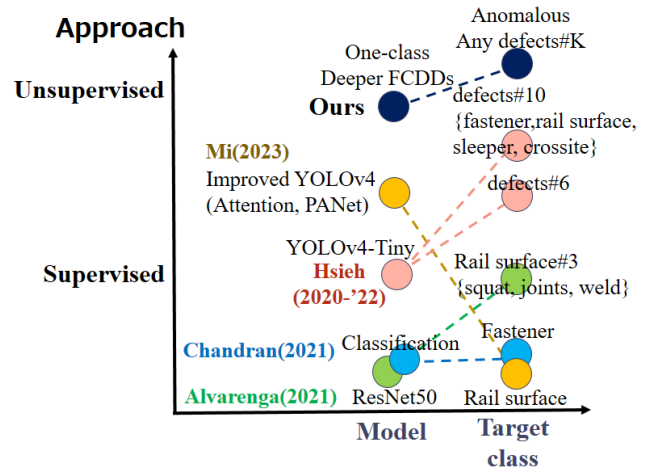


Figure 1. Related models and targets for railway prognostic inspection and our approach.

## 1. INTRODUCTION

### 1.1. Wooden Sleeper, Derailment Risk in Rural Railway

Evans analyzed fatal train accident on Europe's main line railways from 1980 to 2019, and found that the primary cause of accident are train collision, derailment, railroad crossing (Evans, 2011)(Evans, 2020). 1987-2018 derailment statistics in Japan, the traffic safety committee reported 173 cases, whose three main cause contains 65 natural disaster, 47 railroad crossing, and 33 railway infrastructure (Oyama & Miwa, 2022). Based on the cause of railway track, derailment accident has been divided two type : derailment among inter-rail, and ride up on the outside rail. The reason of inter-rail derailment is frequently why decayed wooden sleeper makes weaken the supporting power to spike the rail, so the distance between the parallel rail could expand. Rural railway managers were small scale and severe financial status, where derailment among inter-rail occurred have short length of running operations and minus profit per day kilometers. The rail track structure in rural railway often use wooden sleeper,

so the derailment among inter-rail would be occurred with higher probability. Thus, in rural railway maintenance, monitoring wooden sleeper deterioration is critical task for reducing the risk of derailment. While doing the repair of wooden sleeper or renewal of concrete-sleeper, it often requires a lot of human labors towards a single decayed sleeper for working one by one. Deep learning based visual inspection is able to improve the performance of weekly inspection in rural railway track.

## 1.2. Deep Learning for Visual Railway Inspection

Tang et al reviewed articles on artificial intelligence applications in railway systems from 2010 to 2020 (Tang et al., 2022). The distribution of papers were categorized into five sub-domains: maintenance and inspection, traffic planning and management, safety and security, autonomous driving and control, and passenger mobility. Maintenance and inspection was the most popular research field that had over 81 papers with 57 percent. From a view point of supervised deep learning and recent adoptions to rail industries, Ji et al reviewed the existing deep learning applications to rail track condition monitoring from 2013 to 2021 (Ji, Woo, Wong, & Quek, 2021). Specifically the number of papers surged in 2018, where world-wide 14 regions were represented by rail-related research works. This indicated that the rail industries have been adopting deep learning methods with growing interests. The raw data type was observed that 70 percent of studies used image-type raw data for the deep learning models. The remaining type included acoustic emission signals, defectogram, maintenance records, synthetic data from generative model, and so forth. The purpose of study was observed that detection, classification, and/or localizing rail surface defects including various components such as rail, insulator, valves, fasteners, switches, track intrusions, etc. Over 38 deep learning models were adopted by researchers, where the CNNs have been popular for extracting features and RNN/LSTM has been used for the sequential data type.

It is observed that there is a consistent process flow for deep learning applications to rail track condition monitoring. The first subsystem of image acquisition (cameras/recording devices) is installed on rail engineering maintenance vehicles to capture ray input data. The second subsystem is optional pre-processing that images could be resized, enhanced, noise removed, or cropped for target areas with image processing techniques. And the input data is prepared for the training and testing of deep learning models. Finally, the trained model is put in production with the trained parameters for real-world applications. Because of criticality of rail track condition monitoring, redundancy of inspections by human operators could be provided to double confirm the accuracy. The aforementioned deep applications were based on the supervised learning algorithms with experienced raw images and the annotated labels. However, the nature of rail operations caused

the distribution of rail track image data to be uneven and extremely disproportional, which could cause class imbalance problems. In this paper, we propose an unsupervised learning method using the one-class classification algorithm for a novel application to rail track condition monitoring.

## 1.3. Unsupervised Detection via One-class Classification

As shown in Figure 1, there are several railway inspection applications using deep learning models towards specified defective classes of railway components. These image-based detection applications often use supervised deep learning approach such as classification (Alvarenga et al., 2021), (Chandran, Asber, Thiery, Odelius, & Rantatalo, 2021) and object detection (Mi, Chen, & Zhao, 2023), (Hsieh et al., 2020), (Hsieh, Hsu, & Huang, 2022). In supervised learning studies, the authors have annotated class labels by whole images, and bounding boxes that included with the defective region. Such a defective target of railway components contains rail track, fastener, and sleeper.

Proportionally, railway defect is uncertain event and the number of anomalous images is imbalanced towards the normal class. The defective class is not yet completely defined in railway inspection. For example, Hsieh et al (Hsieh et al., 2020) defined six normal classes and four defective classes focusing on clip on wood/concrete crosstie, spike, fishplate, slide-bed plate, and guard rail plate. Herein, the number of collected real images were limited that seven classes had less than 100 defective images, and three classes had two or more hundreds of images. It is not easy to reconstruct the synthetic images as a health condition on railway components behind the background of complex nature: tree, grass, and ballast stone. Furthermore, it is difficult to generate defective feature as a fruitful annotation data that contributes the performance of architecture.

To build a railway inspection application, collecting defective status data always constraints time consuming for data acquisition, because the temporal occurrence is extremely imbalanced. For stable and high performance, supervised learning approach have to require thousands of paired dataset of defective real images and the annotated class labels or bounding boxes. In contrast, unsupervised anomaly detection approach has a merit that fewer images enables us to optimize the parameters for training normal and anomalous feature. Furthermore, the visual heat map explanation enables us to discriminate the localized defective feature. In this paper, we propose a prognostic discriminator pipeline to automate one-class classification towards defective railway components. We demonstrate our application for railway inspection in an open-accessed dataset of rail track fault, and related steel surface of scratch defects.

## 2. ANOMALY DETECTION, RISK-WEIGHTED SCORE

### 2.1. One-class Classification via Deeper FCDDs

Let  $F_i$  be the  $i$ -th frame of image with a size of  $h \times w$ , and let  $c$  be the center of the hypersphere boundary between the inlier normal region and outlier anomalous region. We consider the number of training images, as well as the weight  $W$  of the FCN. The deep SVDD objective function (Ruff et al., 2018) is formulated as a minimization problem for deep support vector data description as follows:

$$\min_W \frac{1}{n} \sum_{i=1}^n \|\varphi_W^B(F_i) - c\|^2, \quad (1)$$

where denotes the  $\varphi_W^B(F_i)$  mapping of the deeper CNN to the backbone  $B$  based on the input image. The one-class classification model is formulated as follows using the cross-entropy loss function:

$$\begin{aligned} \mathcal{L}_{DeepSVDD} = & -\frac{1}{n} \sum_{i=1}^n (1 - z_i) \log(\ell(\varphi_W^B(F_i))) \\ & + z_i \log[1 - \ell(\varphi_W^B(F_i))], \end{aligned} \quad (2)$$

where  $z_i = 1$  denotes the anomalous label of the  $i$ -th frame of image and  $z_i = 0$  denotes the normal label of the  $i$ -th frame of image. For a more robust loss formulation, the pseudo-Huber loss function was introduced (Ruff, Vandermeulen, Franks, Müller, & Kloft, 2021) in Equation (2). We let  $\ell(u)$  be the loss function and define the pseudo-Huber loss as follows:

$$\ell(u) = \exp(-H(u)), \quad H(u) = \sqrt{\|u\|^2 + 1} - 1. \quad (3)$$

By substituting Equation (2) into Equation (3), we obtain the following expression:

$$\begin{aligned} (2) \equiv & -\frac{1}{n} \sum_{i=1}^n (1 - z_i) H(\varphi_W^B(F_i)) \\ & + z_i \log[1 - \exp\{-H(\varphi_W^B(F_i))\}]. \end{aligned} \quad (4)$$

Therefore, the deeper FCDD loss function can be formulated as follows:

$$\begin{aligned} \mathcal{L}_{deeperFCDD} = & \frac{1}{n} \sum_{i=1}^n \frac{(1 - z_i)}{uv} \sum_{x,y} H_{x,y}(\varphi_W^B(F_i)) \\ & - z_i \log \left[ 1 - \exp \left\{ \frac{-1}{uv} \sum_{x,y} H_{x,y}(\varphi_W^B(F_i)) \right\} \right], \end{aligned} \quad (5)$$

where  $H_{x,y}(u)$  are the elements  $(x, y)$  of the receptive field with a size of  $u \times v$  under the deeper FCDD. The risk-weighted anomaly score  $S_i^{rw}$  of the  $i$ -th image is expressed as the sum of all elements of the receptive field as follows:

$$S_i^{rw}(B) = r_i \sum_{x,y} H_{x,y}(\varphi_W^B(F_i)), \quad i = 1, \dots, n. \quad (6)$$

Here,  $r_i$  is the weight of derailment risk that could be caused by the wooden sleeper deterioration. For example, it can be set that the larger ratio of curve, the higher weight. Exactly, we can provide the  $i$ -th ratio of curve so as to match the GNSS-based position. In this study, we constructed a baseline FCDD with an initial backbone  $B = 0$  and performed CNN27 mapping  $\varphi_W^0(F_i)$  from input frame of image  $F_i$  in a dataset. We also present deeper FCDDs focusing on the elaborate backbones  $B \in \{\text{VGG16, ResNet101, Inceptionv3}\}$  with a mapping operation  $\varphi_W^B(F_i)$  to achieve a more robust detection. We present ablation studies on an dataset in rural railway.

### 2.2. Hazard-mark Heatmap Upsampling Receptive Field

CNN architectures with millions of common parameters have achieved high performance for visual inspection. However, the reasons for their impressive performance remain unclear. To localize the anomalous feature, heatmap visualization techniques can largely be divided into masked sampling and activation map approaches. The former category includes occlusion sensitivity (Zeiler & Fergus, 2013) and local interpretable model-agnostic explanations (Ribeiro, Singh, & Guestrin, 2016). The main merit of this approach is that it does not require in-depth knowledge of network architecture, but its main disadvantage is that it requires iterative computations per image and additional running time for local partitioning, masked sampling, and output prediction.

The last category includes activation maps such as class activation maps (CAMs) (Zhou, Khosla, Lapedriza, Oliva, & Torralba, 2015) and gradient-based extension (Grad-CAM) (Selvaraju et al., 2017). Weighting the feature maps of CAMs is ineffective because it limits global average pooling and full connection effectiveness in the final layer of a CNN. The main advantage of the gradient approach is that it can be applied to any layer of a CNN; therefore, it has significantly improved applicability. However, the main disadvantage is that parallel computation resources and a moderate running time are required for generating a gradient-based heatmap.

For railway inspection applications, we selected the receptive field upsampling approach (Liznerski et al., 2021) to visualize anomalous features using an upsampling-based activation map with Gaussian upsampling from the receptive field of the FCN. The main advantages of the upsampling approach include reduced computational resource requirements and lower running times. The proposed upsampling algorithm generates a full-resolution anomaly heatmap from the input of a low-resolution receptive field  $u \times v$ . Let  $H \in R^{u \times v}$  be a low-resolution receptive field (input), and let  $H' \in R^{h \times w}$  be a full-resolution damage heatmap (output). We define a 2D

Gaussian distribution  $G_2(m_1, m_2, \sigma)$  as follows:

$$[G_2(m_1, m_2, \sigma)]_{x,y} \equiv \frac{1}{2\pi\sigma^2} \exp\left(-\frac{(x-m_1)^2 + (y-m_2)^2}{2\sigma^2}\right). \quad (7)$$

The Gaussian upsampling algorithm from the receptive field is then implemented as follows:

1.  $H' \leftarrow 0 \in R^{h \times w}$
2. for all output pixels  $d$  in  $H \leftarrow 0 \in R^{u \times v}$
3.  $u(d) \leftarrow$  is upsampled from a receptive field of  $d$
4.  $(c_1(u), c_2(u)) \leftarrow$  is the center of the field  $u(d)$
5.  $H' \leftarrow H' + d \cdot G_2(c_1, c_2, \sigma)$
6. end for
7. return  $H'$

Based on the experiments on various datasets, we set the size of the receptive field to  $28 \times 28$  as a practical value. To generate a hazardous heatmap, not like a revealed damage mark, we must unify the display range corresponding to the anomaly scores ranging from the minimum to maximum value. To strengthen the defective regions and highlight the hazard-marks, we define a display range of  $[\min. \max./4]$ , whose quartile parameter is 0.25. Therefore, the histogram of anomaly scores has a long-tailed shape. If we include the complete anomaly score range, then the color would be weakened to blue or yellow on the maximum side.

Table 1. Dataset of rural railway track.

Dataset	Size	Normal	Anomalous
Wooden sleeper (video)	224 <sup>2</sup>	547	435

### 3. APPLIED RESULTS

#### 3.1. Data Preparedness for Rural Railway Prognostics

As summarized in Table 1, we demonstrate a railway-purpose application through an experimental study in rural railway track. The authors prepared the dataset that was acquired using a video camera along a single track in a rural railway with the length of around 80 km in Japan. The video had 30 frames per second, that was too much information to directly use it for learning an anomaly detection model. To overlap each unit of railway track, every 4 frames were skipped into 52 thousand of frame images. And, to reduce the background noise, each 4K frame were cropped into the size of  $1200 \times 1920$ .

For input data preparedness from the cropped images, we have built two classification models using transfer learning based on the ResNet18 and 101. First, there were many locations that contains large shadow or whole dark situations. Then, we built a first classifier using the ResNet18 with

three classes that contains shadow, whole dark, and without shadow. In detail, randomly sampling 3000 from the cropped images, we have annotated into 1458 shadow, 152 whole dark, and 1390 without shadow. The training were set the mini-batch 32 and iterated 15 epochs using Adam, then it resulted in the test accuracy 96.7 percent. We have predicted the 52 thousands of cropped images via the shadow/dark/without classifier, so we have subdivided into 24957 shadow, 2437 whole dark, and 24374 without shadow.

Second, there were lots of grassy spots on the ballast track, wooden sleeper, and outside of track in each frame image. Then, we built a second classifier using the ResNet101 with three classes that includes grassy, decayed wood-sleeper, and normal without grass. Exactly, randomly sampling 1500 from the 24374 cropped images without shadow, we have annotated into 270 grassy, 435 decayed wood-sleeper, and 547 normal without grass. The training were set the mini-batch 128 and iterated 15 epochs using Adam, then it resulted in the test accuracy 66.4 percent. We have predicted the randomly sampled 8000 images without shadow using the grassy/decayed wooden sleeper/normal classifier, so we have subdivided into 1184 grassy, 2787 decayed wooden sleeper, and 4029 normal without grass. For space restriction, another opportunity remains for the 8000 sampling. In this paper, the authors use the annotated 435 decayed wooden sleeper and 547 normal without grass for ablation studies. Finally, when we were training our model using the both dataset, the size of input images were resized to  $224^2$ .

#### 3.2. Training the Anomaly Detector and Accuracy

The input size was set to  $224^2$  while training the anomaly detector. We set the mini-batch size to 32 and number of epochs to 300. We used the Adam optimizer with a learning rate of 0.0001, set the gradient decay factor to 0.9, and set the squared gradient decay factor to 0.99. The training images were partitioned to set a ratio of 65:15:20 for the numbers of training, calibration, and testing images, respectively. As shown in Table 2, the VGG16 based deeper FCDDs have outperformed the baseline and other backbone based deeper FCDDs on the rural railway dataset.

Table 2. Backbone ablation studies on defective detection using our proposed deeper FCDDs for Wooden sleeper (video).

Backbone	AUC	$F_1$	Precision	Recall
CNN27	0.6577	0.5093	0.5540	0.4712
<b>VGG16</b>	<b>0.7970</b>	<b>0.6831</b>	<b>0.6000</b>	<b>0.7931</b>
ResNet101	0.7756	0.6699	0.5798	0.7931
Inceptionv3	0.7940	0.6700	0.6000	0.7586

#### 3.3. Hazard-mark Heatmaps for Railway Prognostics

We visualized damage features using the Gaussian upsampling of the receptive field of our deeper FCDD network. We

also generated a histogram of the anomaly scores of test images for railway defective dataset. Figure 2 shows the hazard-mark explanation based on the VGG16 backbone. The red region in the heatmap successes to recognize the decayed wooden sleeper. In contrast, there are some false negative from background noise. Figure 4 reveal that several overlapping bins exist in the horizontal anomaly scores. Therefore, the score range is moderately separated for decayed wood-sleeper inspection in rural railway track.

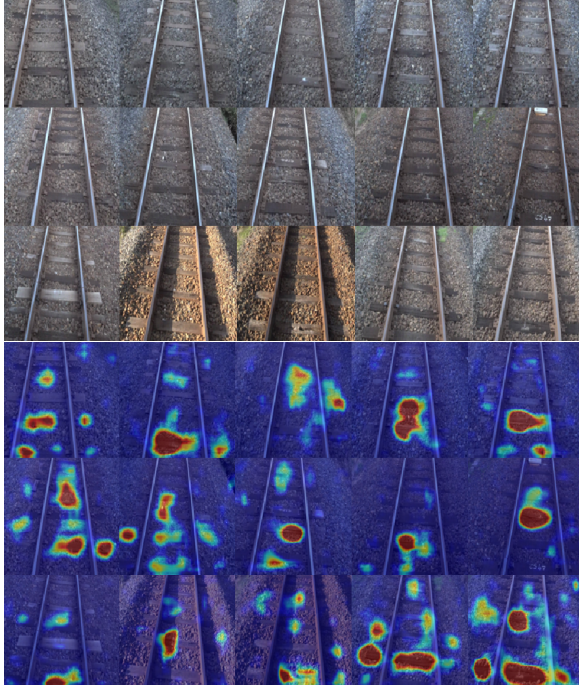


Figure 2. Input raw images (left) and damage mark heatmaps (right) of decayed wood-sleeper based on VGG16 backbone.

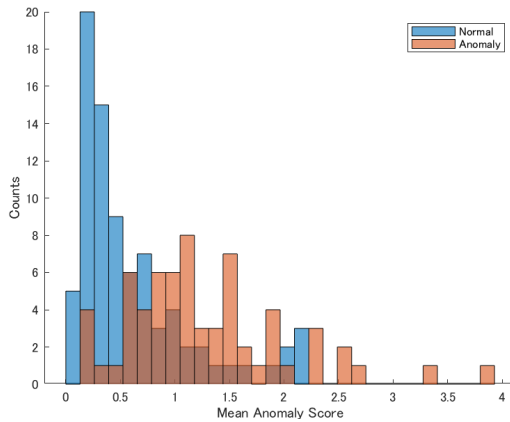


Figure 3. Histogram of decayed wood-sleeper scores corresponding to our deeper FCDD on VGG16 backbone.

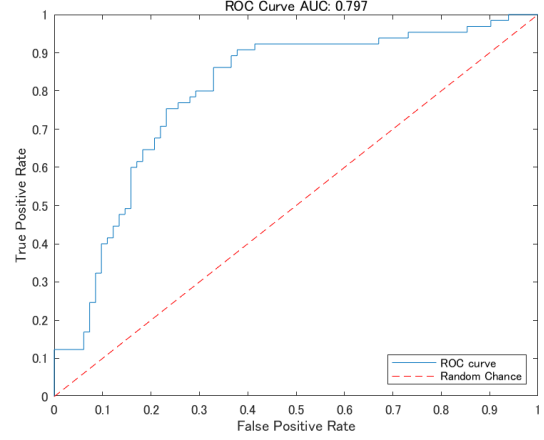


Figure 4. Area Under Curve of decayed wooden sleeper corresponding to our deeper FCDD on VGG16 backbone.

## 4. CONCLUDING REMARKS

### 4.1. Wooden Sleeper Inspection for Railway Prognostics

We constructed a railway-purpose application to automate one-class anomaly detection reproducing a baseline FCDD with a light backbone CNN network containing 27 layers with either Conv-BN-ReLU or Maxpooling activation. To develop a robust application, we evaluated a novel solution of deeper FCDDs with pre-trained backbones of VGG16, ResNet101, and Inceptionv3, and performed ablation studies via comparisons with a baseline FCDD. We propose an index of risk weighted anomaly score to support a making decision to repair the sleeper for reducing the probability of derailment to be safe railway operations. We also visualized hazard-mark heatmaps using direct Gaussian upsampling of the receptive field of the FCN. We evaluated the baseline FCDD model on some experimental targets, namely railway track fault, and decayed wooden sleeper. Herein, the heatmap means that the hazard-marks of decayed wooden sleeper could cause spike out of rail and in worst case, the running train could be occurred derailment. Our experiments yielded higher accuracy of AUC and recall. Without annotating decayed wood-sleeper regions, the deeper FCDDs enhanced hazard-marks for visual explanation. We have found that a hazard localized solution of deeper FCDDs outperformed the baseline FCDD on the rural railway datasets. A novel solution of deeper FCDDs provides a wooden sleeper damage detection tool for rural railway inspection utilized in the higher accuracy, hazard-explainability.

### 4.2. Future Works for Risk-based Maintenance

Several promising directions exist for future works to develop more usable and visual inspection applications. For more robust training in the presence of background noise and defective class imbalance, an augmentation preprocessing operation could be effective for one-class classification models,

e.g. mixup, and random erasing. The imbalanced issue remains for data mining non-frequent defects: spike out of rail from wooden sleepers, crack of concrete sleeper, and hole on ballast track. For effective data acquisition of rare classes, risk weighted anomaly score using our deeper FCDDs could be used at edge devices. Instead of collecting all frame images, specified hazard-marked frames that have a significantly higher anomaly score than a predefined threshold could be efficiently collected. We have a data scaling opportunity to annotate and train the remained dataset of over 5000 images that we have classified into 2000 decayed wooden sleeper, and 3000 normal without grass. To incorporate the potential hazard of derailment in each track, we are able to add the label of curve ratio (Oyama & Miwa, 2022). Then, we can utilize the risk-weighted anomaly score for supporting to make a decision of priority to repair effectively for sustainable and safety operation in rural railway.

#### ACKNOWLEDGMENT

The authors wish to thank MathWorks and Takuji Fukumoto, who provided helpful MATLAB resources for automated visual inspection. We also thank Nakasha Creative Co.,Ltd., who provided an opportunity of studies for rural railway.

#### REFERENCES

- Alvarenga, T. A., Carvalho, A. L., Honorio, L. M., Cerqueira, A. S., Filho, L. M. A., & Nobrega, R. A. (2021). Detection and classification system for rail surface defects based on eddy current. *Sensors*, 21(23).
- Chandran, P., Asber, J., Thiery, F., Odelius, J., & Rantatalo, M. (2021). An investigation of railway fastener detection using image processing and augmented deep learning. *Sustainability*, 13(21).
- Evans, A. W. (2011). Fatal train accidents on Europe's railways: 1980–2009. *Accident Analysis and Prevention*, 43(1), 391–401.
- Evans, A. W. (2020). *Fatal train accidents on Europe's railways: 1980–2019* (Tech. Rep.). Centre for Transport Studies, Imperial College London.
- Hsieh, C.-C., Hsu, T.-Y., & Huang, W.-H. (2022). An online rail track fastener classification system based on YOLO models. *Sensors*, 22(24).
- Hsieh, C.-C., Lin, Y.-W., Tsai, L.-H., Huang, W.-H., Hsieh, S.-L., & Hung, W.-H. (2020). Offline deep-learning-based defective track fastener detection and inspection system. *Sensors and Materials*, 32(10), 3429.
- Ji, A., Woo, W. L., Wong, E. W. L., & Quek, Y. T. (2021). Rail track condition monitoring: A review on deep learning approaches. *Intelligence and Robotics*, 1(2), 151–175.
- Liznerski, P., Ruff, L., Vandermeulen, R. A., Franks, B. J., Kloft, M., & Müller, K.-R. (2021). Explainable deep one-class classification. In *The international conference on learning representations (ICLR)*.
- Mi, Z., Chen, R., & Zhao, S. (2023). Research on steel rail surface defects detection based on improved YOLOv4 network. *Frontiers in Neurorobotics*, 17.
- Miwa, M. (2019). Railway maintenance transformed by Numerical Optimizer. In *Mathematical systems user conference 2019*.
- Oyama, T., & Miwa, M. (2022). Applying probabilistic mathematical modeling approach and ai technique to investigate serious train accidents in japan. *Sustainability Analytics and Modeling*, 2, 2667–2596.
- Ribeiro, M. T., Singh, S., & Guestrin, C. (2016). "why should i trust you?": Explaining the predictions of any classifier. In *Proceedings of the 22nd ACM SIGKDD international conference on knowledge discovery and data mining* (p. 1135–1144). Association for Computing Machinery.
- Ruff, L., Vandermeulen, R., Goernitz, N., Deecke, L., Siddiqui, S. A., Binder, A., ... Kloft, M. (2018, 10–15 Jul). Deep one-class classification. In J. Dy & A. Krause (Eds.), *Proceedings of the 35th international conference on machine learning* (Vol. 80, pp. 4393–4402). PMLR.
- Ruff, L., Vandermeulen, R. A., Franks, B. J., Müller, K.-R., & Kloft, M. (2021). Rethinking assumptions in deep anomaly detection. In *The international conference on machine learning (ICML)*.
- Selvaraju, R. R., Cogswell, M., Das, A., Vedantam, R., Parikh, D., & Batra, D. (2017). Grad-CAM: Visual explanations from deep networks via gradient-based localization. In *2017 IEEE international conference on computer vision (ICCV)* (p. 618–626).
- Tang, R., De Donato, L., Besinovic, N., Flammini, F., Goverde, R. M., Lin, Z., ... Wang, Z. (2022). A literature review of artificial intelligence applications in railway systems. *Transportation Research Part C: Emerging Technologies*, 140, 103679.
- Zeiler, M. D., & Fergus, R. (2013). *Visualizing and understanding convolutional networks*.
- Zhou, B., Khosla, A., Lapedriza, A., Oliva, A., & Torralba, A. (2015). *Learning deep features for discriminative localization*.

#### BIOGRAPHIES

**Takato Yasuno** (ORCID: 0000-0002-4796-518X) He received his D.E. degree from Tottori University. He has 23 years of experience in 128 consulting projects as civil engineer for asset management planning. Since 2017, he works in the Research Institute for Infrastructure Paradigm Shift (RIIPS) as a senior researcher at the Yachiyo Engineering Co.,Ltd (YEC). He is a member of the Japanese Society for Artificial Intelligence (JSAI). He has over 20 articles that contains machine learning methodologies and applied results for



civil and natural disaster applications. His research interest contains in data mining and machine learning, automated civil inspection for diagnosis/prognostics, damage detection.

**Masahiro Okano** He graduated the Japan Electronics College for data science and development and operations (DevOps) regarding AI systems. He has experience in building deep neural network architecture and deploying civil and environmental applications. He works in the RIIPS as a researcher at YEC. He is a member of the JSAI. His research interest includes prompt design and fewer-shot prediction using foundation models for civil engineering.

**Junichiro Fujii** He received his B.E degree from Kyoto University and M.A.S. (Interdisciplinary Information Studies) degree from University of Tokyo. He has over 20 years of experience in information systems development. He works in the RIIPS as the chief of AI analysis Team at YEC. He is a member of the JSAI. His research interest is applying artificial intelligence to the field of civil engineering.

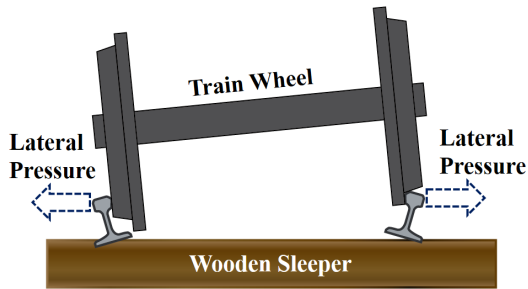


Figure 5. Derailment inside track

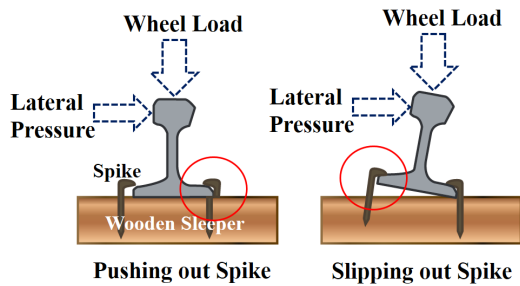


Figure 6. Pushing out and slipping out spike on the wooden sleeper

## APPENDIX

### Spike on Decayed Wooden Sleeper

Derailment accident has been divided two types : derailment inside track, and riding up outside rail. As shown in Fig-

ure 5, that is illustrated with reference to (Miwa, 2019), one of cause of derailment inside track is why decayed wooden sleeper makes strengthen the lateral pressure, and the distance between the parallel rails could expand. As shown in Figure 6, that is drawn with reference to (Miwa, 2019), longitudinal wheel load and lateral pressure makes pushing out or slipping out the spike on wooden sleeper. Decayed wooden sleeper accelerate to be anomalous status of spike.

### Noise Reduction Classification in Data-preparedness

As shown in Figure 7, test images of predicted examples by our first classifier for shadow noise reduction. Herein, we built a classification model using the ResNet18 with three classes that contains shadow, whole dark, and without shadow. As shown in Figure 8, test images of pre-



Figure 7. Cropped images of predicted results by first trained classifier with 3 classes: shadow/dark/without based on the ResNet18.

dicted examples by our second classifier for grass noise reduction. Herein, we built a classification model using the ResNet101 with three classes that includes grassy, decayed wooden sleeper, and normal without grass.

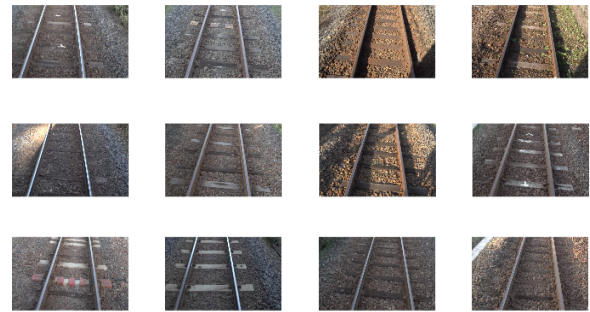


Figure 8. Cropped images of predicted results by second trained classifier with 3 classes: the grassy/decayed wood sleeper/normal class based on ResNet101.